Contribution from the Department of Chemistry,
William Marsh Rice University, Houston, Texas 77001

Magnetic and Spin Lifetime Studies in Solution of a $\Delta S = 1$ Spin-Equilibrium Process for Some Six-Coordinate Bis(*N*-R-2,6-pyridinedicarboxaldimine)cobalt(II) Complexes[1]

MIRIAM G. SIMMONS[2] and LON J. WILSON*

Received June 24, 1976 AIC604512

Five pseudooctahedral ^{2}E(low-spin) $\rightleftarrows$ ^{4}T(high-spin) spin-equilibrium bis(*N*-R-2,6-pyridinedicarboxaldimine)cobalt(II) complexes with R = $C(CH_3)_3$, $CH(CH_3)_2$, $NH(CH_3)$, *p*-$PhCH_3$, and CH_2Ph have been synthesized as PF_6^- salts and studied in both the solid and the solution states. Variable-temperature magnetic susceptibility measurements (solid, 77–300 K; solution, 200–300 K) reveal considerable differences in behavior of the ^{2}E(ls) $\rightleftarrows$ ^{4}T(hs) processes in the two environments. In solution the rates of

$$^2\text{E(ls)} \underset{k_{-1}}{\overset{k_1}{\rightleftarrows}} {}^4\text{T(hs)}$$

intersystem crossing for the R = $NH(CH_3)$ derivative have been measured, in collaboration with Dr. Norman Sutin, by laser Raman temperature-jump kinetics. First-order rate constants in CH_3CN/CH_3OH for the forward (k_1) and reverse (k_{-1}) steps are 3.2×10^6 and 9.1×10^6 s^{-1} with the corresponding spin state lifetimes, $\tau(^2\text{E})$ and $\tau(^4\text{T})$, being 3.1×10^{-7} and 1.1×10^{-7} s, respectively. Rate constants and spin lifetimes for this one-electron spin change ($\Delta S = 1$) have been compared to available data characterizing $\Delta S = 2$ processes in several pseudooctahedral iron(II) and iron(III) complexes.

Introduction

In the last few years there has been a renewed interest in the study of the electronically unusual spin-equilibrium phenomenon in transition metal complexes. Much of our recent interest[3-7] has focused on the solution state since (1) unpredictable solid-state lattice effects influencing the spin equilibrium are effectively factored out, (2) "dynamic"

$$\text{low-spin (ls)} \underset{k_{-1}}{\overset{k_1}{\rightleftarrows}} \text{high-spin (hs)}$$

interconversion processes can be assumed, and (3) first-order rate constants (k_1 and k_{-1}) and spin state lifetimes [τ(spin state) = k^{-1}] can, in principle, be directly measured by rapid perturbation kinetics such as the laser Raman temperature-jump[8] or ultrasonic relaxation[9] techniques. Such spin state lifetime studies are of fundamental importance in transition metal chemistry for understanding intersystem crossing phenomena in photochemical excited states and in laying the ground work for directly investigating the role of spin multiplicity changes on electron-transfer rates and specificity in both variable-spin inorganic and metalloprotein systems.[10,11] To date, solution magnetic and spin state lifetime studies of this nature have been limited to pseudooctahedral complexes of Fe(II) [^{1}A(ls) $\rightleftarrows$ ^{5}T(hs) for O_h symmetry][7,8] and Fe(III) [^{2}T(ls) $\rightleftarrows$ ^{6}A(hs)],[5,6] both of which involve a two-electron ($\Delta S = 2$) spin interconversion. In this work we report the first such complete solution characterization and study of a $\Delta S = 1$ Co(II) [^{2}E(ls) $\rightleftarrows$ ^{4}T(hs)] spin-equilibrium process. The family of complexes which have been investigated are those of the bis(*N*-R-2,6-pyridinedicarboxaldimine)cobalt(II) class shown in Figure 1 with R = $C(CH_3)_3$, $CH(CH_3)_2$, $NH(CH_3)$, *p*-$PhCH_3$, and CH_2Ph.

Experimental Section

Physical Measurements. Solid-state magnetic susceptibilities were measured by the Faraday method using a Cahn Model 6600-1 research magnetic susceptibility system. The cryogenics consisted of an Air Products Faraday Interface Model DMX-19 vacuum shroud, an LT-3-110B Heli-tran system, and a APD-TL digital temperature readout monitoring an iron-doped gold vs. chromel thermocouple. $Hg[Co(NCS)_4]$ was used as the calibrant. Pascal's constants were used to correct for ligand and PF_6^- diamagnetism in 10^{-6} cgsu: $C(CH_3)_3$ compound, −417; $CH(CH_3)_2$ compound, −392; $NH(CH_3)$ compound, −331; *p*-$PhCH_3$ compound, −505; CH_2Ph compound, −500; PF_6^-, −64. Solution magnetic moments were determined by the Evans ^{1}H NMR method[12] with methanol and ethylene glycol being used for temperature calibration. The measurements were corrected for sample concentration and solvent density changes with temperature.[13] Chloroform was used as the internal reference compound.

Solid-state infrared spectra were obtained in the region 4000–600 cm^{-1} using NaCl plates and Nujol mulls. A Model 31 YSI conductivity bridge was used to obtain solution conductivities. ^{1}H NMR spectra were run at 60 MHz on a Varian A56/60A spectrometer modified for isotropic shift studies or a Perkin-Elmer R12 spectrometer. UV–VIS spectra were run on a Cary 17 using jacketed quartz cells; the temperature was monitored with a thermistor and all values are ±0.5 °C.

Relaxation curves for the R = $NH(CH_3)$ spin-equilibrium compounds were obtained in solution using the laser-stimulated Raman temperature-jump technique previously described.[8,14] An CH_3CN/CH_3OH solution (1:4 by volume) was used and data were obtained at 25 °C in a thermostated (±1 °C) cell. The relaxation traces obtained from photographs of oscilloscope displays measured the change in optical density of the sample spectrum with time at 400 nm. The first-order relaxation time, τ, in nanoseconds for the

$$^2\text{E} \underset{k_{-1}}{\overset{k_1}{\rightleftarrows}} {}^4\text{T}$$

spin-interconversion process was determined from log ($I_\infty - I$) vs. time plots generated from the photographs. The final τ = 83 ns value used resulted from eight separate lasing experiments on the same sample; the estimated error is 23 ns. The equilibrium constant, K_{eq} ($=k_1/k_{-1}$), was obtained from solution magnetic susceptibility measurements, with the value used being 0.35 at 25 °C. Rate constants, k_1 and k_{-1}, for the spin interconversion processes were calculated from the measured relaxation time ($\tau^{-1} = k_1 + k_{-1}$) and the known equilibrium constant. The spin state lifetimes, $\tau(^2\text{E})$ and $\tau(^4\text{T})$, are then simply k_1^{-1} and k_{-1}^{-1}, respectively.

Materials and Syntheses. The 2,6-pyridinedicarboxaldehyde was prepared by MnO_2 oxidation of 2,6-pyridinedimethanol as previously reported,[15] except that the MnO_2 was washed only with $CHCl_3$ (not ether), and the product recrystallized from ether and heptane. The MnO_2 was prepared as reported by Mancera et al.,[16] except that it was washed only with hot (90 °C) water instead of ether or CH_3OH. The brown MnO_2, thus obtained, can be kept in a tightly stoppered bottle for months without loss of activity. The 2,6-pyridinedicarboxaldehyde was obtained in 20% yield; mp 121 °C (lit. mp 124 °C). Predominant ir peaks (Nujol mull): 1730, 1310, 1210, 810, and 780 cm^{-1}.

The reagent grade primary amines were purchased from Aldrich Chemical Co. Spectroquality acetone and CH_3OH, reagent grade CH_3CN and DMSO, and practical grade CH_3NO_2 were used for the studies. Elemental chemical analyses were obtained commercially.

All compounds were prepared, as their PF_6^- salts, by the same general method, which follows. To 2 mmol of 2,6-pyridinedicarboxaldehyde dissolved in 25 ml of CH_3OH, 4 mmol of the appropriate amine was added dropwise, except for *p*-toluidine which was added directly as the solid. A yellow solution resulted immediately.

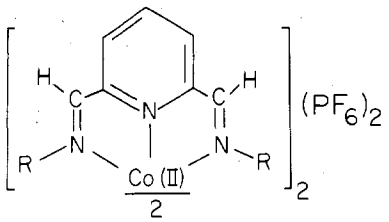

Figure 1. The $^2E \rightleftarrows {}^4T$ bis(*N*-R-2,6-pyridinedicarboxaldimine)cobalt(II) hexafluorophosphate compounds with R = $C(CH_3)_3$, $CH(CH_3)_2$, $NH(CH_3)$, *p*-$PhCH_3$, and CH_2Ph.

One millimole of $CoCl_2 \cdot 6H_2O$ was then added as a crystalline solid, yielding an intensely colored solution in all cases. To this solution 5 mmol of KPF_6 dissolved in 50 ml of warm CH_3OH was then added with filtration. After addition of the KPF_6, which usually initiated precipitation, the solution was taken to dryness at room temperature under reduced pressure. The resulting solid was extracted into 50 ml of dry acetone to remove inorganic salts and crystallization of the $[Co(N\text{-R-2,6-pyridinedicarboxaldimine})_2](PF_6)_2$ compound from the acetone solution was induced by cooling and the slow addition of anhydrous ether. The products were recrystallized from an acetone–ether mixture, collected by filtration, and dried under vacuum over P_2O_5 at 1 Torr for a minimum of 12 h.

The R = $C(CH_3)_3$ compound was obtained as a light green solid in 87% yield. Anal. Calcd for $CoC_{30}H_{46}N_6P_2F_{12}$: Co, 7.02; C, 42.91; H, 5.53; N, 10.01. Found: Co, 6.91; C, 42.87; H, 5.52; N, 9.80. Λ_c = 268 Ω^{-1} cm^{-1} for a 10^{-3} M acetone solution at 30 °C. Electronic spectrum in CH_3OH: peak maximum at 305 nm ($\epsilon \sim 16\,000$) with shoulder at 360 nm ($\epsilon \sim 2000$).

The R = $CH(CH_3)_2$ compound was obtained as a brick red solid in 75% yield. Anal. Calcd for $CoC_{26}H_{38}N_6P_2F_{12}$: Co, 7.52; C, 39.85; H, 4.90; N, 10.73. Found: Co, 7.49; C, 39.79; H, 4.86; N, 10.56. Λ_c = 266 Ω^{-1} cm^{-1} for a 10^{-3} M acetone solution at 30 °C. Electronic spectrum in CH_3OH: peak maximum at 295 nm ($\epsilon \sim 16\,000$) with a shoulder at 375 nm ($\epsilon \sim 2000$).

The R = $NH(CH_3)$ compound was obtained as a light brown powder in 80% yield. Anal. Calcd for $CoC_{18}H_{26}N_{10}P_2F_{12}$: Co, 8.07; C, 29.55; H, 3.56; N, 19.15. Found: Co, 8.07; C, 29.64; H, 3.38; N, 19.24. Λ_c = 265 Ω^{-1} cm^{-1} for a 10^{-3} M acetone solution at 30 °C. Electronic spectrum in CH_3OH: peak maximum at 290 nm ($\epsilon \sim 51\,000$) with a shoulder at 365 nm ($\epsilon \sim 12\,000$).

The R = *p*-$PhCH_3$ compound was obtained as a rust red solid in 60% yield. Anal. Calcd for $CoC_{42}H_{38}N_6P_2F_{12}$: Co, 6.05; C, 51.69; H, 3.90; N, 8.61. Found: Co, 6.08; C, 51.68; H, 3.88; N, 8.60. Λ_c = 273 Ω^{-1} cm^{-1} for a 10^{-3} M acetone solution at 30 °C. Electronic spectrum in CH_3OH: peak maximum at 335 nm ($\epsilon \sim 20\,000$) with a shoulder at 560 nm ($\epsilon \sim 750$).

The R = CH_2Ph compound was obtained as a light red solid in 71% yield. Anal. Calcd for $CoC_{42}H_{38}N_6P_2F_{12}$: Co, 6.05; C, 51.69; H, 3.90; N, 8.61. Found: Co, 6.28; C, 50.95; H, 3.88; N, 8.39. Λ_c = 250 Ω^{-1} cm^{-1} for a 10^{-3} M solution in acetone at 30 °C. Electronic spectrum in CH_3CN: peak maximum at 285 nm ($\epsilon \sim 10\,500$) with shoulders at 380 nm ($\epsilon \sim 1900$) and 560 nm ($\epsilon \sim 950$).

Variable-Temperature Susceptibility Data (T in K, χ_m' in 10^{-6} cgsu mol^{-1}, μ_{eff} in μ_B). R = $C(CH_3)_3$ compound (solid): 304.0, 11 218, 5.24; 252.2, 13 122, 5.17; 208.9, 14 742, 4.98; 155.7, 18 853, 4.87; 101.1, 25 268, 4.54; 78.3, 32 328, 4.52.

R = $C(CH_3)_3$ compound (acetone): 334.2, 9798, 5.14; 310.2, 10 143, 5.04; 304.2, 10 470, 5.07; 285.2, 10 553, 4.93; 263.7, 11 644, 4.98; 249.7, 12 126, 4.94; 238.2, 12 629, 4.93; 217.7, 14 056, 4.96; 208.2, 14 926, 5.01.

R = $CH(CH_3)_2$ compound (solid): 297.8, 6631, 3.99; 280.0, 6245, 3.76; 265.0, 6042, 3.59; 251.2, 5687, 3.39; 240.0, 5483, 3.26; 227.6, 5226, 3.10; 210.0, 4764, 2.84; 182.5, 4236, 2.50; 150.0, 3865, 2.16; 130.3, 4151, 2.09; 111.3, 4451, 2.00; 91.7, 5065, 2.00; 77.7, 6204, 2.00.

R = $CH(CH_3)_2$ compound (acetone): 332.2, 7600, 4.52; 312.2, 7450, 4.33; 303.2, 7056, 4.15; 273.2, 6815, 3.88; 255.7, 6494, 3.66; 236.7, 5953, 3.37; 224.7, 5640, 3.20; 208.2, 4860, 2.87; 200.7, 4947, 2.83; 192.2, 4441, 2.62.

R = $NH(CH_3)$ compound (solid): 296.0, 1988, 2.18; 231.2, 2217, 2.03; 182.5, 2824, 2.04; 117.3, 4672, 2.00; 79.2, 5993, 2.00.

R = $NH(CH_3)$ compound (acetone): 333.2, 4549, 3.50; 298.7, 4029, 3.12; 285.2, 3955, 3.02; 273.2, 3955, 2.93; 255.7, 3587, 2.72; 236.7, 3291, 2.51; 224.7, 3104, 2.37; 208.2, 3043, 2.26; 200.7, 2951, 2.10.

R = $NH(CH_3)$ compound (CH_3CN): 334.2, 4694, 3.56; 308.2, 4397, 3.31; 295.7, 4057, 3.11; 277.2, 3963, 2.98; 259.7, 3750, 2.80; 246.2, 3438, 2.61; 241.2, 3384, 2.56; 224.7, 3169, 2.40.

R = $NH(CH_3)$ compound (CH_3OH): 319.2, 4444, 3.38; 310.2, 4390, 3.31; 302.7, 3968, 3.11; 272.2, 3522, 2.78; 248.2, 2993, 2.45; 223.7, 2737, 2.22; 188.2, 2827, 2.07.

R = $NH(CH_3)$ compound (CH_3NO_2): 319.2, 4064, 3.23; 310.2, 4068, 3.19; 302.7, 3680, 3.00; 272.2, 3597, 2.81; 248.2, 2924, 2.42.

R = *p*-$PhCH_3$ compound (solid): 296.9, 9634, 4.99; 275.0, 9856, 4.67; 242.0, 10 368, 4.52; 227.4, 10 948, 4.50; 185.5, 13 251, 4.47; 138.5, 16 298, 4.28; 101.5, 20 111, 4.12; 78.5, 25 128, 3.99.

R = *p*-$PhCH_3$ compound (acetone): 333.2, 7311, 4.43; 309.2, 7084, 4.20; 292.7, 6684, 3.97; 271.2, 6387, 3.74; 248.2, 5907, 3.44; 229.7, 5305, 3.13; 213.2, 4924, 2.91.

R = *p*-$PhCH_3$ compound (CH_3OH): 311.2, 4816, 3.48; 271.5, 4355, 3.09; 249.7, 4543, 3.02; 234.7, 4029, 2.88; 183.15, 4081, 2.46.

R = *p*-$PhCH_3$ compound (CH_3CN): 315.2, 7923, 4.49; 295.7, 7756, 4.30; 267.2, 7262, 3.96; 249.7, 6770, 3.69; 228.2, 6037, 3.33.

R = *p*-$PhCH_3$ compound (CH_3NO_2): 315.2, 7149, 4.25; 295.7, 6974, 4.08; 267.2, 6750, 3.81; 255.7, 6512, 3.66.

R = CH_2Ph compound (solid): 297.4, 7681, 4.29; 272.4, 7837, 4.14; 255.2, 7704, 3.98; 196.5, 7699, 3.49; 153.7, 7763, 3.10; 127.7, 7888, 2.85; 106.5, 8128, 2.64; 82.3, 8961, 2.44.

R = CH_2Ph compound (CH_3CN): 334.2, 5275, 3.77; 306.2, 4739, 3.42; 295.7, 4669, 3.34; 285.2, 4445, 3.20; 277.2, 4637, 3.22; 263.2, 4318, 3.05; 248.2, 4122, 2.87; 241.2, 3896, 2.75; 236.2, 3872, 2.72; 232.2, 4003, 2.74; 224.7, 3743, 2.61.

Results and Discussion

Magnetic Properties and Structural Considerations. All of the bis(*N*-R-2,6-pyridinedicarboxaldimine)cobalt(II) complexes synthesized and studied in this work as their PF_6^- salts are new except for a R = CH_2Ph iodide salt[17] derivative which has previously been reported to be a $^2E \rightleftarrows {}^4T$ spin-equilibrium compound in the solid state. In addition, several other R derivatives, not reported here, such as the R = CH_3,[18] NH_2,[19] and C_2H_5 and C_6H_5 compounds,[20] have been synthesized, but of these only the R = NH_2 compound has been studied for its anomalous spin-equilibrium magnetic behavior in the solid state.[17] To our knowledge, however, no systematic studies of these Co(II) $^2E \rightleftarrows {}^4T$ spin equilibria in solution have previously appeared, although a solution-state spin equilibrium has been documented for the structurally similar $[Co(terpy)_2]^{2+}$ complex.[8,21]

Available analytical and solution conductivity data, as reported in the Experimental Section, are consistent with the bis(tridentate) monomeric nature of the bis(*N*-R-2,6-pyridinedicarboxaldimine)cobalt(II) cations as shown in Figure 1. The μ_{eff} vs. T curves (77–300 K) for the series in the solid state are shown in Figure 2B as a function of the R substituent. The actual data are listed in the Experimental Section. Depending on the R substituent, the Co(II) centers at room temperature exhibit μ_{eff} values spanning the entire ^2E low-spin (1.9–2.0 μ_B) to ^4T high-spin (4.7–5.2 μ_B) range with the R = $C(CH_3)_3$ (5.24 μ_B at 304 K) and R = $NH(CH_3)$ (2.18 μ_B at 296 K) derivatives being near the limiting high-spin and low-spin values, respectively. The remaining three derivatives, R = $CH(CH_3)_2$, CH_2Ph, and *p*-$PhCH_3$, exhibit intermediate magnetic moments at room temperature which display the anomalous non-Curie temperature dependency characteristically associated with Co(II) $^2E \rightleftarrows {}^4T$ spin equilibria, having the spin-crossover region around room temperature.[22] All of the μ_{eff} vs. T curves appear continuous and are devoid of the sharp discontinuities that are known to sometimes accompany spin-equilibrium processes in the solid phase.[3,23]

Variable-temperature solution magnetic data (200–300 K) for the series in acetone are shown in Figure 2A where it is seen that all of the derivatives, except for the R = $C(CH_3)_3$ species, exhibit a pattern of decreasing μ_{eff} values with temperature which is consistent with the preservation of the spin-equilibrium phenomenon in the solution state. While these

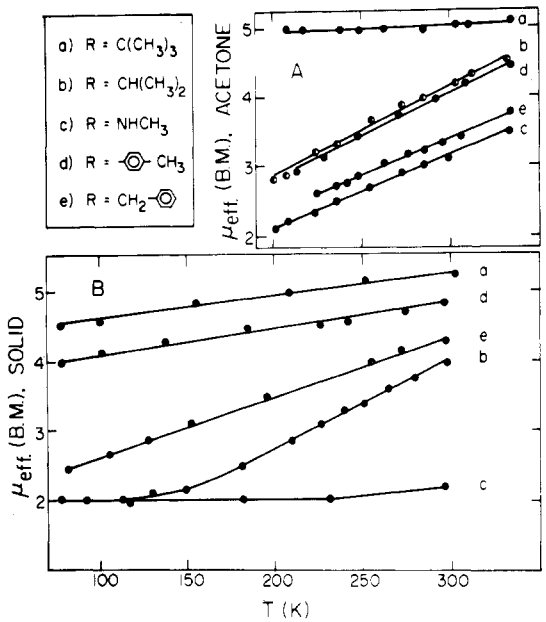

Figure 2. μ_{eff} vs. temperature curves for the bis(*N*-R-2,6-pyridinedicarboxaldimine)cobalt(II) hexafluorophosphate salts in acetone (A) and as solids (B).

magnetic data demonstrate the existence of the $^2E \rightleftarrows {}^4T$ spin-equilibrium phenomenon in solution, they also serve to emphasize that solid-state magnetic data cannot be used a priori to infer solution behavior since, as shown in Figure 2, (1) the $C(CH_3)_3$ derivative is a $^2E \rightleftarrows {}^4T$ compound in the solid state but not in solution, (2) the $NH(CH_3)$ derivative is a $^2E \rightleftarrows {}^4T$ compound in solution but essentially only low spin in the solid state, and (3) the relative "ordering" of the $CH(CH_3)_2$, *p*-$PhCH_3$, and CH_2Ph compounds differs in the two environments. Such solution vs. solid discrepancies are not, however, particularly surprising in view of the fact that it has been recently shown[5,6] that such subtle effects as [(metal complex)···solvent] hydrogen-bonding interactions can drastically influence the equilibrium position of ls $\rightleftarrows$ hs solution processes. In fact, these Co(II) $^2E \rightleftarrows {}^4T$ processes also appear somewhat solution dependent with, for example, the high-spin state for the $NH(CH_3)$ compound being favored according to the solvent sequence $(CH_3)_2SO > CH_3CN \sim$ acetone $> CH_3OH > CH_3NO_2$.

In solution the percent high-spin character for the present spin-equilibrium series increases according to the R group ordering $C(CH_3)_3 > CH(CH_3)_2 >$ *p*-$PhCH_3 > CH_2Ph > NH(CH_3)$. This ordering is undoubtedly a composite reflection of both R group electronic and steric consequences. However, space-filling molecular models indicate that steric considerations probably play a dominant role in these complexes. For the most sterically demanding R = $C(CH_3)_3$ group, models show that the greater high-spin character of this compound is promoted by *intra*molecular nonbonding interactions between the R methyl groups of one pyridinedicarboxaldimine ligand and the pyridine π network of the second ligand. An increase in the Co–N bond distances to minimize these steric interactions apparently decreases *Dq* sufficiently to stabilize the high-spin ^4T state as the ground state for the R = $C(CH_3)_3$ compound. On the other hand, less sterically demanding R substituents presumably permit shorter Co–N distances with sufficiently strong ligand fields to produce the ^2E(ls) state as the ground state with a low-lying thermally accessible ^4T(hs) state also being available. The presence of such a steric mechanism determining the spin-equilibrium property in these $^2E \rightleftarrows {}^4T$ complexes is further evidenced by ^1H NMR isotropic shift data for the R = $C(CH_3)_3$ compound in acetone at room temperature which consists of eight signals ranging from −173 to +150 ppm from external TMS. Assuming that three of the resonances are due to the methine and pyridine meta and para protons, the remaining five must be assigned to stereochemically nonequivalent methyl protons of rotationally "locked" methyl groups resulting from the CH_3–pyridine ring steric contact interactions. A temperature-dependent study (202–317 K) did not produce any change in the spectrum multiplicity and a $\Delta\nu$(iso) vs. T plot of the −32.5-ppm (room temperature) signal was found to be linear and Curie in behavior, with increasing shifts from TMS with decreasing temperature. In contrast, a similar plot of the −27.5-ppm (room temperature) peak for the spin-equilibrium R = $NH(CH_3)$ compound deviated from this expected Curie pattern, exhibiting decreasing shifts from TMS with decreasing temperature.

Table I. Thermodynamic Parameters for the Co(II) $^2E \rightleftarrows {}^4T$ Spin-Equilibrium Processes in the Solid and Solution States

R	Medium	$\Delta H°$,[a,b] kcal mol^{-1}	$\Delta S°$,[a,b] eu
$C(CH_3)_3$	Solid	1.38 ± 0.65	13.80 ± 3.24
$CH(CH_3)_2$	Solid	2.43 ± 0.20	8.29 ± 0.90
	Acetone	2.37 ± 0.10	8.45 ± 0.37
$NH(CH_3)$	Acetone	2.70 ± 0.06	6.95 ± 0.25
	MeOH	3.26 ± 0.14	8.64 ± 0.53
	CH_3CN	2.61 ± 0.08	6.71 ± 0.29
	CH_3NO_2	3.23 ± 0.35	8.32 ± 1.18
p-$PhCH_3$	Solid	0.34 ± 0.10	3.55 ± 0.44
	Acetone	2.85 ± 0.18	9.15 ± 0.71
	MeOH	1.53 ± 0.10	3.54 ± 0.41
	CH_3CN	2.69 ± 0.06	10.07 ± 0.20
	CH_3NO_2	2.16 ± 0.07	7.67 ± 0.26
CH_2Ph	Solid	0.79 ± 0.08	3.20 ± 0.38
	CH_3CN	2.27 ± 0.09	6.11 ± 0.33

[a] Determined from magnetic susceptibility data (with standard deviations), assuming $K_{eq} = [^4T]/[^2E]$ and $\mu_{eff}(^4T) = 5.2\ \mu_B$ and $\mu_{eff}(^2E) = 2.0\ \mu_B$ as the limiting high-spin and low-spin values, respectively. [b] Temperature intervals used in calculating parameters are as listed in variable-temperature susceptibility data section in the Experimental Section.

The $\Delta H°$ and $\Delta S°$ thermodynamic parameters characterizing the $^2E \rightleftarrows {}^4T$ spin equilibria, as derived from their temperature-dependent equilibrium constants, are shown in Table I. The method used in calculating the parameters has been previously described.[3] In general, the parameters obtained from the solution variable-temperature magnetic measurements are judged to be the more useful for discussion purposes, since, in the solid, unpredictable lattice effects (phase changes, anion dependence, hysteresis) are known to sometimes obscure the true electronic structure within the spin-crossover region; this view is further supported by the data in the table where the parameters for a given compound, as derived from solid- and solution-state data, usually differ to a much larger degree than those obtained in solution where only the solvent is varied.

The calculated $\Delta H°$(solution) values in Table I range from 1.53 to 3.26 kcal mol^{-1} with the major contribution to $\Delta H°$ likely arising from the changing Co–N bond distances and energies which are known to accompany spin-conversion processes. The positive $\Delta H°$'s demonstrate the ^2E(ls) state to be the lower energy state in these complexes. Although no structural data, viz., those from variable-temperature crystallography, are yet available for these or any other $^2E \rightleftarrows {}^4T$ one-electron interconversion ($\Delta S = 1$) spin-equilibrium compounds,[33] it is reasonable that the low-spin $^2E(t_{2g}^6e_g^*)$ form will possess shorter Co–N distances, and therefore greater Co–N bond strengths, than the high-spin $^4T(t_{2g}^5e_g^{*2})$ form. In cases where variable-temperature structural data are available, as for the two $\Delta S = 2$ Fe(II) species [Fe(6-

Table II. Spin-Interconversion Kinetics Data for Low-Spin $\underset{k_{-1}}{\overset{k_1}{\rightleftharpoons}}$ High-Spin Processes in Solution

Compd	Spin-transition type	Exptl conditions	k_1, s^{-1} [τ(ls), s]	k_{-1}, s^{-1} [τ(hs), s]	Ref
$[Fe^{III}(Sal)_2trien]^+$	d^5; $^2T \rightleftarrows {}^6A$; $\Delta S = 2$	CH_3OH; 20 °C	1.5×10^7 [6.7×10^{-8}]	1.4×10^7 [7.1×10^{-8}]	5
$[Fe^{III}(acac)_2trien]^+$	d^5; $^2T \rightleftarrows {}^6A$; $\Delta S = 2$	Acetone/CH_3OH; 25 °C	1.5×10^7 [6.7×10^{-8}]	6.9×10^6 [1.5×10^{-7}]	6
$[Fe^{II}(polypyrazolylborate)_2]^0$	d^6; $^1A \rightleftarrows {}^5T(^5A)$; $\Delta S = 2$	CH_3OH/CH_2Cl_2; 21 °C	1.0×10^7 [1.0×10^{-7}]	2.0×10^7 [5.0×10^{-8}]	8
$[Fe^{II}(6\ Mepy)_2(py)tren]^{2+}$	d^6; $^1A \rightleftarrows {}^5T(^5A)$; $\Delta S = 2$	Acetone/CH_3OH; 20 °C	4.0×10^6 [2.5×10^{-7}]	5.0×10^6 [2.0×10^{-7}]	7
$[Co^{II}(N\text{-}NH(CH_3)\text{-}2,6\text{-}pyAld)_2]^{2+}$	d^7; $^2E \rightleftarrows {}^4T$; $\Delta S = 1$	CH_3CN/CH_3OH; 25 °C	3.2×10^6 [3.1×10^{-7}]	9.1×10^6 [1.1×10^{-7}]	This work

Mepy)$_3$tren]$^{2+}$ [3] and [Fe(bpy)$_2$(NCS)$_2$],[24] the average Fe–N distances have been found to decrease by 0.12–0.25 Å upon a high-spin $^5T(t_{2g}^4e_g^{*2}) \rightarrow$ low-spin $^1A(t_{2g}^6)$ spin conversion. Similarly, for the $\Delta S = 2$ Fe(III) complex [Fe(Et$_2$dtc)$_3$],[25] the six Fe–S bond distances have also been shown to decrease, but by only ~0.11 Å for a complete high-spin $^6A(t_{2g}^3e_g^{*2}) \rightarrow$ low-spin $^2T(t_{2g}^5)$ spin transition process. Thus, available data indicate that primary coordination sphere reorganization for variable-spin $\Delta S = 2$ processes involve changes in the average metal–ligand bond distances of ~0.10–0.25 Å. For a Co(II) $\Delta S = 1$ case, the corresponding high-spin → low-spin geometry change is predicted to be smaller, since the spin transition involves only a single- rather than a two-electron depopulation of the e_g^* orbital set. Of course, other factors, such as *intra*molecular ligand–ligand nonbonding stereochemical interactions, could serve to modify the extent of such structural alterations so that geometry changes for $\Delta S = 1$ and $\Delta S = 2$ processes might actually be more similar than predicted on these electronic grounds alone. Only detailed crystallographic studies on these and other variable-spin systems hold some hope of unraveling the relative importance of these electronic and stereochemical contributions to the geometry changes accompanying spin-conversion processes.

Assuming that $\Delta H°$(solution) values for these spin equilibria largely reflect the changing metal–ligand bond distances and energies which accompany the spin-interconversion process, it was of interest to attempt a comparison of the $\Delta S = 1$ and $\Delta S = 2$ processes by way of this parameter. Relatively few spin equilibria have yet been documented and studied in solution with the only available $\Delta H°$(solution) values (i.e., for acetone) being for the $^1A \rightleftarrows {}^5T$ Fe(II) species [Fe(polypyrazolylborate)$_2$]^0 ($\Delta H°$ = 3.9 kcal mol^{-1}),[26] [Fe(6-Mepy)(py)$_2$tren]$^{2+}$ ($\Delta H°$ = 4.6 kcal mol^{-1}),[3] and [Fe(6-Mepy)$_2$(py)tren]$^{2+}$ ($\Delta H°$ = 2.8 kcal mol^{-1}),[3] the $^2T \rightleftarrows {}^6A$ Fe(III) species [Fe(Me$_2$dtc)$_3$]^0 ($\Delta H°$ = 1.6 kcal mol^{-1}),[27] [Fe(XSal)$_2$trien]$^+$ ($\Delta H°$ = 3.5–5.9 kcal mol^{-1}),[5] [Fe(acac)$_2$trien]$^+$ ($\Delta H°$ = 2.0 kcal mol^{-1}),[6] [Fe((acacCl)$_2$trien)]$^+$ ($\Delta H°$ = 2.2 kcal mol^{-1}),[6] and [Fe(bzac)$_2$trien]$^+$ ($\Delta H°$ = 2.5 kcal mol^{-1}),[6] and the present $^2E \rightleftarrows {}^4T$ Co(II) species ($\Delta H°$ = 2.3–2.9 kcal mol^{-1}). While the $\Delta H°$(solution) values for the $\Delta S = 1$ Co(II) complexes fall near the low end of the range spanned by the available data, they are not otherwise distinguished. The $\Delta S°$ parameters in Table I partially reflect an electronic entropy change of R ln 3 or 2.18 eu expected for these $^2E \rightleftarrows {}^4T$ phenomena, with the remaining contribution probably arising from configurational entropy[34] associated with the geometrical changes in the Co–N_6 core occurring with the transition and solvent sphere reorganization accompanying the spin-induced geometry change. Thus, a solvent dependency on $\Delta S°$, as observed, is not surprising.

Measurement of ^2E and ^4T Spin State Lifetimes. The temperature dependency of the UV–VIS electronic spectrum for the $^2E \rightleftarrows {}^4T$ R = NH(CH$_3$) derivative in CH_3OH is shown in Figure 3. Judging from the band intensities (as listed in the Experimental Section), all bands are metal → ligand charge transfer in origin, and a careful search at lower energies revealed no low-intensity bands of purely "d–d" character. The spectral changes with temperature for this spin-equilibrium process in solution are much less dramatic than that displayed by some recently reported variable-spin Fe(II)[3,4,7,8] and Fe(III)[5,6] systems and are more reminiscent of the small temperature effects observed in the spectrum of the $^2T \rightleftarrows {}^6A$ tris(dithiocarbamato)iron(III) complexes.[28] For this reason the Fe(dtc)'s and present Co(II) complexes do not exhibit the marked thermochromism often found to be characteristic of the spin-equilibrium phenomenon. Most of the spectral change with temperature in Figure 3 has been attributed to the changing low-spin and high-spin isomer populations where μ_{eff} decreases from 3.05 μ_B at 295 K (23% hs; 77% ls) to 2.30 μ_B at 231 K (6% hs; 94% ls); however, some of the observed temperature dependency may simply be due to band sharpening at low temperatures, since even the spin-invariant R = C(CH$_3$)$_3$ compound displays this tendency.

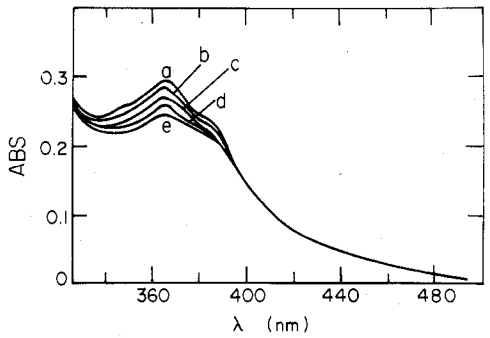

Figure 3. Variable-temperature electronic spectrum for the R = NH(CH$_3$) derivative in CH_3OH at (a) 231 K, (b) 245 K, (c) 261 K, (d) 268 K, and (e) 295 K; [complex] ≈ 10^{-3} M.

To measure the kinetics of the

$$^2E \underset{k_{-1}}{\overset{k_1}{\rightleftharpoons}} {}^4T$$

intersystem-crossing process in the R = NH(CH$_3$) compound, the laser Raman temperature-jump technique, developed at Brookhaven, has been employed.[14] To date only the R = NH(CH$_3$) compound has been thus studied with the entire series of spin-equilibrium compounds to be examined in future work. The instrumentation and data collection and treatment are described in the Experimental Section. The solvent medium chosen for the study was CH_3CN/CH_3OH (1:4 by volume) with CH_3CN being used to facilitate compound solubility and CH_3OH being used to produce effective stimulated Raman heating of the sample solution. A typical relaxation curve for the R = NH(CH$_3$) compound at 25 °C, as monitored at 400 nm, is shown in Figure 4. The fully high-spin R = C(CH$_3$)$_3$ compound was also examined at

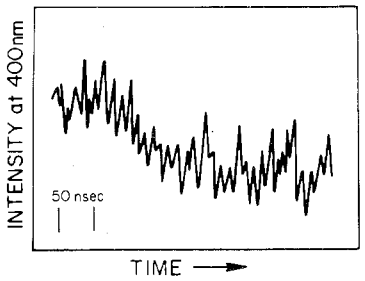

Figure 4. Laser Raman temperature-jump relaxation trace obtained for the R = $NH(CH_3)$ derivative in CH_3CN/CH_3OH solution at 25 °C; [complex] ≈ 10^{-3} M.

several wavelengths, with no evidence of a relaxation process being observed. This result strongly supports the contention that the observed relaxation for the R = $NH(CH_3)$ compound is indeed due to an intramolecular spin-equilibrium process between the two ^2E and ^4T energy levels, as characterized above. Therefore, the observed relaxation has been analyzed in terms of a first-order exponential time dependence for a $^2E \rightleftarrows {}^4T$ spin interconversion process. The low signal intensity shown in Figure 4 is undoubtedly a combined result of the fact that $\Delta H°$ is relatively small ($\lesssim$3 kcal mol^{-1}) for this spin-interconversion process and that the electronic spectral changes with temperature are also small.

Forward and reverse rate constants, k_1 and k_{-1}, for the $\Delta S = 1$ spin interconversion process are shown in Table II, along with similar results which have been reported for four representative $\Delta S = 2$ iron processes. Also shown in the table are the corresponding spin state lifetimes where $\tau(ls) = k_1^{-1}$ and $\tau(hs) = k_{-1}^{-1}$. Considering the diverse collection of metal ion electronic structures and ligand types found in the table, the measurable spin state lifetimes span a surprisingly narrow range of $\sim 5 \times 10^{-8}$ to 3×10^{-7} s. Attempts to measure spin-interconversion rates for other systems not reported in Table II, such as for $[Co^{II}(terpy)_2]^{2+}$,[29] $[Fe^{III}(Me_2dtc)_3]^0$,[6] and $[Fe^{III}(bzac)_2trien]^+$,[6] have not been successful because the relaxation times appear shorter than the heating rise time of the experiment ($\tau \leq 30$ ns).[30] From electronic considerations alone it seems reasonable that Co(II) $\Delta S = 1$ processes, with their expected smaller coordination sphere reorganization, might exhibit larger k's and shorter τ(spin state)'s than those for the $\Delta S = 2$ iron systems, and, indeed, this may be true for the $[Co(terpy)_2]^{2+}$ complex.[29] However, this is not the case for the present Co(II) R = $NH(CH_3)$ derivative. In fact, spin-interconversion rates for this $\Delta S = 1$ process are among the slowest of those listed in Table II. This fact, along with the similarities in all the measured lifetimes, regardless of the metal ion electronic structure, suggests that *nonelectronic factors* may be rate determining in these spin-interconversion processes. For example, if the rate-determining step involves a primary coordination sphere and secondary solvent sphere reorganization as a prerequisite to the spin transition itself, $\Delta S = 1$ and $\Delta S = 2$ events would appear kinetically indistinguishable for similar reorganizational processes and rate of spin transition >> rate of reorganization.[31] If this interpretation is correct, it may be possible to significantly modify spin-interconversion rates and lifetimes by appropriate ligand design or solvent medium selection. In this manner spin-conversion rates might be sufficiently retarded so as to become competitive with fast outer-sphere electron-exchange reactions, such as for the $[Fe(6\text{-}Mepy)_2(py)tren]^{2+}$–$[Fe(6\text{-}Mepy)_2(py)tren]^{3+}$ or $[Fe(bpy)_3]^{2+}$–$[Fe(bpy)_3]^{3+}$ couples where k(exchange) is likely to be $\gtrsim 10^5$ s^{-1}.[32]

Acknowledgment. We gratefully acknowledge the Robert A. Welch Foundation (Grant C-627) and the Petroleum Research Fund, administered by the American Chemical Society, for financial support of this work. In addition, we wish to express our thanks to Mr. Michael Tweedle and Dr. Mitchell A. Hoselton for assistance in the laser temperature-jump experiments and to Dr. Norman Sutin for the use of the equipment.

Registry No. $[Co^{II}(N\text{-}C(CH_3)_3\text{-}2,6\text{-}pyAld)_2](PF_6)_2$, 60676-11-1; $[Co^{II}(N\text{-}CH(CH_3)_2\text{-}2,6\text{-}pyAld)_2](PF_6)_2$, 60645-71-8; $[Co^{II}(N\text{-}NH(CH_3)\text{-}2,6\text{-}pyAld)_2](PF_6)_2$, 60645-73-0; $[Co^{II}(N\text{-}p\text{-}PhCH_3\text{-}2,6\text{-}pyAld)_2](PF_6)_2$, 60645-75-2; $[Co^{II}(N\text{-}CH_2Ph\text{-}2,6\text{-}pyAld)_2](PF_6)_2$, 60686-60-4.

References and Notes

(1) Presented in part at the Centennial National Meeting of the American Chemical Society, New York, N.Y., April 1976; see Abstracts, No. INOR 47.
(2) Robert A. Welch Foundation Graduate Fellow.
(3) M. A. Hoselton, L. J. Wilson, and R. S. Drago, *J. Am. Chem. Soc.*, **97**, 1722 (1975).
(4) L. J. Wilson, D. Georges, and M. A. Hoselton, *Inorg. Chem.*, **14**, 2968 (1975).
(5) M. F. Tweedle and L. J. Wilson, *J. Am. Chem. Soc.*, **98**, 4824 (1976).
(6) E. V. Dose, K. M. M. Murphy, and L. J. Wilson, *Inorg. Chem.*, **15**, 2622 (1976).
(7) M. A. Hoselton, R. S. Drago, L. J. Wilson, and N. Sutin, *J. Am. Chem. Soc.*, **98**, 6967 (1976).
(8) J. K. Beattie, N. Sutin, D. H. Turner, and G. W. Flynn, *J. Am. Chem. Soc.*, **95**, 2052 (1973).
(9) W. P. Mason, *Phys. Acoust.*, **2A**, 203–279 (1965).
(10) M. C. Palazzotto and L. H. Pignolet, *Inorg. Chem.*, **13**, 1781 (1974).
(11) J. K. Beattie and R. J. West, *J. Am. Chem. Soc.*, **96**, 1933 (1974), and references therein.
(12) D. F. Evans, *J. Chem. Soc.*, 2003 (1959).
(13) D. Ostfeld and I. A. Cohen, *J. Chem. Educ.*, **49**, 829 (1972).
(14) D. H. Turner, G. W. Flynn, N. Sutin, and J. V. Beitz, *J. Am. Chem. Soc.*, **94**, 1554 (1972).
(15) E. P. Papadopoulos, A. Jarrar, and C. H. Issidorides, *J. Org. Chem.*, **31**, 615 (1966).
(16) O. Mancera, G. Rosenkranz, F. Sondheimer, and M. Urquiza, *J. Am. Chem. Soc.*, **77**, 4145 (1955).
(17) R. C. Stoufer, D. W. Smith, E. A. Clevenger, and T. E. Norris, *Inorg. Chem.*, **5**, 1167 (1966).
(18) P. E. Figgens and D. H. Busch, *J. Am. Chem. Soc.*, **82**, 820 (1960).
(19) R. C. Stoufer and D. H. Busch, *J. Am. Chem. Soc.*, **78**, 6016 (1956).
(20) F. Lions and K. V. Martin, *J. Am. Chem. Soc.*, **79**, 2733 (1957).
(21) J. S. Judge and W. A. Baker, Jr., *Inorg. Chim. Acta*, **1**, 68 (1967).
(22) See, for example, D. L. Williams, D. W. Smith, and R. C. Stoufer, *Inorg. Chem.*, **6**, 590 (1967).
(23) W. A. Baker and H. M. Bobonich, *Inorg. Chem.*, **3**, 1184 (1964).
(24) E. König and K. J. Watson, *Chem. Phys. Lett.*, **6**, 457 (1970).
(25) J. G. Leipoldt and P. Coppens, *Inorg. Chem.*, **12**, 2269 (1973).
(26) J. P. Jesson, S. Trofimenko, and D. R. Eaton, *J. Am. Chem. Soc.*, **89**, 3158 (1967).
(27) Unpublished results.
(28) Unpublished results; A. H. Ewald, I. G. Ross, and A. H. White, *Proc. R. Soc. London, Ser. A*, **280**, 235 (1964).
(29) See ref 8, footnote 9.
(30) It may be possible to observe relaxation times for these processes by ultrasonic relaxation techniques which are theoretically capable of measuring τ's down to ~3 ns: J. K. Beattie, private communication. Attempts at these measurements are currently under way: J. K. Beattie, to be submitted for publication.
(31) Rate constants of 10^6–10^7 s^{-1} do not seem unreasonable for such processes, especially in view of the $\sim 5 \times 10^5$ s^{-1} values recently reported for the planar $\rightleftarrows$ tetrahedral isomerization, and accompanying singlet $\rightleftarrows$ triplet spin change, in $[Ni(dpp)Cl_2]$: J. J. McGarvey and J. Wilson, *J. Am. Chem. Soc.*, **97**, 2531 (1975).
(32) E. Eichler and A. C. Wahl, *J. Am. Chem. Soc.*, **80**, 4145 (1958).
(33) Recently, a single-temperature structure determination for a spin-equilibrium bis(terpyridyl)cobalt(II) thiocyanate dihydrate derivative has been reported: C. L. Raston and A. H. White, *J. Chem. Soc., Dalton Trans.*, 7 (1976). Also see E. N. Maslen, C. L. Raston, and A. H. White, *ibid.*, 1803 (1974).
(34) E. Konig and G. Ritter, *Mössbauer Eff. Methodol.*, **9**, 3 (1974).